



Brief communication

Characterization and classification of fluidization regimes by non-linear analysis of pressure fluctuations

F.X. Llauró, M.F. Llop *

Department of Chemical Engineering, Agriculture and Food Technology, University of Girona, Avda. Lluís Santaló s/n 17003, Girona, Spain

Received 29 November 2005; received in revised form 15 June 2006

1. Introduction

In spite of the fact that most fluidization applications operate in bubbling regime and many fluidized beds have been developed to operate in turbulent flow, slug flow can appear in some industrial fluidized beds. Numerous studies have been carried out to characterize the fluidization regimes. Several methods have been used, and most of them are based on bubble velocity, bed voidage and pressure fluctuations. However, methods based on more sophisticated techniques have been proposed, such as optical probes (Bai et al., 1999), laser beams (Villa and Guardiola, 2003) and tomography (Makkawi and Wright, 2002). The method based on pressure fluctuations is one of the most popular methods, as it is simple and easy to implement in industrial facilities, and has been demonstrated to be accurate, containing enough information to characterize fluidized bed behaviour (Zijerveld et al., 1998; Bai et al., 1999).

The most widely used method to analyse pressure fluctuations uses linear tools, time domain (standard deviation) and the frequency domain (power spectral density function); however, as the fluidized bed dynamics can be interpreted as deterministic chaos, non-linear tools have also been used. The non-linear analysis of a time series of pressure fluctuations from fluidized beds has been demonstrated to be an excellent tool for characterizing fluidization dynamics; for this reason, many researchers have focused their attention on the chaotic approach to study the behaviour of fluidization regimes (Zijerveld et al., 1998; Bai et al., 1999; Johnsson et al., 2000; Ellis et al., 2003).

The study of chaotic dynamics in fluidized beds is based on the reconstruction of the attractor, which can be reconstructed from experimental data using the embedding theory (Takens, 1981; Daw and Hallow, 1993). The appropriate space dimension and delay must be known, but the delay value determined as described in literature is uncertain and affects the quality of the reconstructed attractor.

Here, we characterize the bubbling, slugging and turbulent flow regimes by analysing the non-linear dynamics of the pressure fluctuations measured in two different beds. New delay-independent invariants have been introduced to characterize the attractor by analysing its evolution with variation of the delay, using metric parameters. This technique should be distinguished from chemometrics, which is based on multivariate techniques such as principal component analysis (PCA) or partial least-squares (PLS) (Esbensen et al., 1998).

* Corresponding author. Tel.: +34 72 418457; fax: +34 72 418399.
E-mail address: miquel.llop@udg.es (M.F. Llop).

Finally, in order to validate and extend the methodology to analysis of the data from other facilities, the procedure has been used to characterize and classify the flow regimes studied by [Johnsson et al. \(2000\)](#).

2. Background

Deterministic dynamic systems are described by the evolution of their variables over time, and can be defined by ordinary differential equations. The system can also be defined by a time-series of any state variable $x(t)$ measured at equal intervals of time.

The system can be represented in its state space of m dimensions, state variables, and the representation of the sequence of each state is called the trajectory. This trajectory can be attracted toward a region of space, in which case it becomes an attractor. It defines the state, or assembly of states, of the system at infinite time and corresponds to the geometric structures that characterize the behaviour of the system in the state space (phase space). As the attractor defines the state of the system, it is assumed that it can characterize the fluidization behaviour and the fluidization regimes adequately.

The phase space trajectories, or the attractor, of a dynamic system can be reconstructed from a single time series using original experimental data and copies of them delayed in time according to the Embedding Theorem ([Takens, 1981](#)). The time series of the pressure fluctuations in the fluidized bed with dimension n and a period of Δt can be expressed as:

$$x(t) = \{x(t_1), x(t_2), x(t_3), \dots, x(t_n)\}. \quad (1)$$

This vector can be unfolded in a pseudo-state-space, Euclidean space m -dimensional (R^m), to generate N points ($N = n - (m - 1)\tau$), where $\tau = k\Delta t$. The reconstructed trajectory is generated by connecting these points.

By choosing carefully the appropriate values for the embedding dimension (m) and the delay time (τ), the reconstructed state space represents an image of the original state. The dynamic properties of both the original and reconstructed state space are the same, having the same invariants (correlation dimension, Lyapunov exponents, Kolmogorov entropy, etc.).

According to this method, reconstructing the state vector consists simply of ascertaining the embedding dimension and the time delay. However, determining these parameters is not easy. The embedding dimension can be calculated using the global false nearest neighbours analysis ([Abarbanel, 1996](#)). The calculation of the delay is not obvious, but it must be calculated because it affects the quality of the attractor ([Roux et al., 1983](#)). [Fraser and Swinney \(1986\)](#) proposed the first minimum of the mutual information function as the best delay to choose. Nevertheless, this method is uncertain, since the minimum does not always appear ([Daw and Hallow, 1993](#)). Moreover, it depends on the number of bins used, chosen arbitrarily to evaluate the mutual information function ([Karamavruç and Clark, 1997](#)).

As the reconstructed state space depends greatly on the arbitrary calculation of the delay, it is advisable to use another more robust methodology to analyse the non-linear characteristics of the pressure time series. The proposed methodology consists of introducing the delay as a variable, generating a different attractor for each delay and characterizing its evolution by a defined shape descriptor ([Annunziato and Abarbanel, 1999](#)).

Geometric moments have been used to describe the shape evolution of the reconstructed attractor, defined as a function of the Euclidean distance selected, as:

$$M_{m,j}(\tau) = \frac{\sum_{i=1}^N d_{m,i}^j}{N}, \quad (2)$$

where $d_{m,i}^j$ is the distance, i is every point of the attractor, j is the moment order, m identifies the distance class, N is the vector length and τ is the delay. In this work, $j = 2, 3, 4$ and $m = 1, 2, \dots, 6$. The even order moments describe attractor dispersion and the odd order moments describe the symmetry. The Euclidean distances used are defined in [Table 1](#). For instance, for $m = 1$, the distance is with respect to the bisector of the first–third quadrant (principal axis), and for $m = 2$ the distance is with respect to the bisector of the second and fourth quadrant (secondary axes). The analysis in this work is limited to two and three dimensions, but the study can be generalized to more dimensions.

Table 1
Distances defined to calculate the moments

Distance	Expression ($d_{m,i}$)
Bisector, 1–3	$d_{1,i} = \frac{1}{\sqrt{2}}(x_i - y_i)$
Bisector, 2–4	$d_{2,i} = \frac{1}{\sqrt{2}}(x_i + y_i)$
Origin	$d_{3,i} = \sqrt{x_i^2 + y_i^2}$
Plane B, $x + y + z = 0$	$d_{4,i} = \frac{1}{\sqrt{3}}(x_i + y_i + z_i)$
Plane C, $x + y - 2z = 0$	$d_{5,i} = \frac{1}{\sqrt{6}}(x_i + y_i - 2z_i)$
Origin	$d_{6,i} = \sqrt{x_i^2 + y_i^2 + z_i^2}$

By increasing the delay, the moments follow a dynamic evolution from $\tau = 0$ (linear system) to higher delay values (non-linear system). The calculation of the corresponding moments as well as the generation of the reconstructed attractor have been done using algorithms implemented in MATLAB.

3. Experimental

The experiments were carried out with two different set-ups. The first was a fluidization column with a diameter of 5 cm and a total height of 1.5 m operating at ambient pressure and room temperature with an 8 cm bed height of settled particles. This set-up was used to obtain the experimental data for the bubbling and turbulent regimes. The fluidization air was supplied at 20 °C by a compressor. The second facility, used for bubbling and slugging regimes, was a column with a diameter of 7.6 cm and a height of 60 cm with a 13 cm bed of settled particles. This facility, which operated in vacuum conditions, was used to achieve the slugging regime by decreasing the operating pressure. Hence, it was not necessary to change either the bed geometry or the particle diameter for this purpose. The influence of vacuum on gas fluidization behaviour has been studied by Llop and Jand (2003). A vacuum pump was used to induce the fluidization airflow through the bed at 20 °C and pressures within the range 4–101.3 kPa. The gas fluidization flow-rate was measured with a sheet of rotameters and regulated with a needle valve.

Both columns were of glass to allow visual observation. Two piezoresistive differential pressure transducers with a response time of 0.005 s (200 Hz) were used to measure the pressure fluctuations. Two pressure probes were located vertically inside the bed connected to the respective transducer, one was closed to the distributor and the other was about 90 mm above the first. The second connection of both transducers was opened to the freeboard. For more details of this experimental set up, see Llop et al. (1996), and Llop and Jand (2003).

The signals from the two transducers were acquired with a personal computer, converted in a 12 bits A/D board and stored. At least 4096 data values were obtained for each differential pressure time series with a frequency of 100 Hz. The solid particles fluidized were silica sand particles of mean diameter 225 μm and 475 μm , with a density of 2650 kg/m^3 , and fluid catalytic cracking (FCC) particles of 50 μm diameter and density of 1700 kg/m^3 .

4. Results and discussion

The moments have been calculated for all the operation conditions analysed (gas velocities and solid particle diameter) operating in the different flow regimes. The moment evolution $M_{1,4}$ for bubbling and slugging regimes is shown in Fig. 1. It can be observed that the evolution of the moments due to the attractor unfolding depends strongly on the delay region considered for both regimes analysed. For low delay values, the moment increases when the delay increases up to a maximum, then it decreases to reach a more or less constant value.

The first phase indicates the start of unfolding of the attractor structure. After the maximum ($M_{1,4}$) is reached, the attractor starts the degenerative process and loses coherence. This general observation for all the moments evaluated suggests that in this first zone the real unfolding process is produced, and the first maximum is the transition in which the attractor evolution is inverted. In general, we observed that the range of

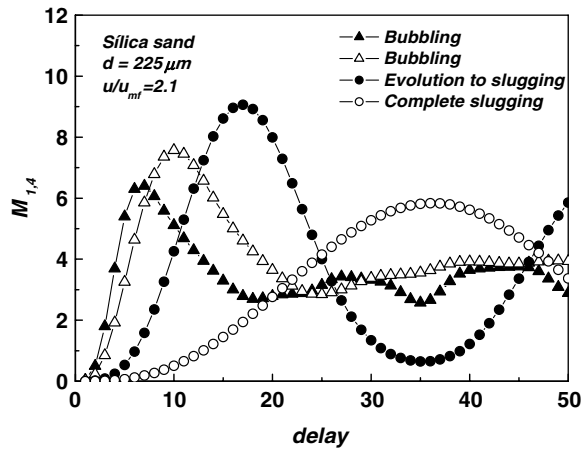


Fig. 1. Evolution of moments $M_{1,4}$ versus the delay for silica sand particles from bubbling to slugging regimes.

the transition from unfolding to degenerative process is very similar for a given flow regime and independent of the moment analysed.

As Fig. 1 shows, the unfolding evolution depends strongly on the flow regime. The evolution of each moment is characteristic, and very different evolution patterns have been observed, depending on the moments studied. For the bubbling regime, the first phase finishes at delay values between 5 and 10. The moment evolution in the slugging regime has a strong periodic component and the first maximum is observed at higher delay values, from 20 to about 40. This evolution indicates that there is an alternative unfolding and folding process. The degenerative process is much slower and it is not evident, at least at moderate delay values. The periodic component seems to be attenuated only at very high delay values. This attenuation is stronger or weaker, depending on the moment.

In other cases, the moment was found to decrease and, after reaching a minimum, it increases with the delay to finally reach a constant value.

The evolution of moment $M_{4,2}$ is plotted in Fig. 2, which shows that, from the bubbling to the turbulent regime, the moment decreases with increases of the delay at the same gas velocity. The minimum is located between a delay of 5 and 10, and the periodic component is stronger in the turbulent regime than in the bubble regime, but weaker than the previously observed slugging regime. This behaviour could be justified by the characteristic evolution from bubbling to turbulent fluidization. From the bubbling regime, the slugging

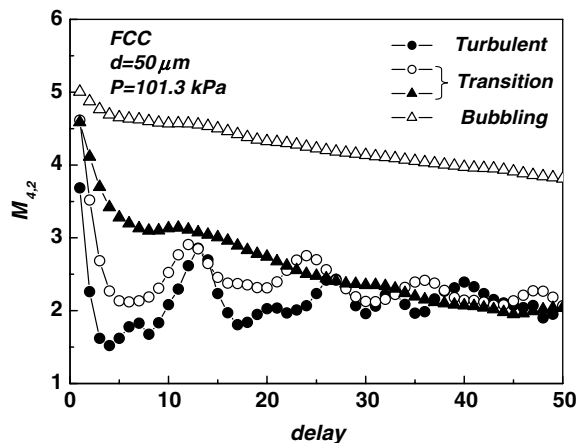


Fig. 2. Evolution of moment $M_{4,2}$ versus the delay from bubbling to turbulent regime for FCC particles.

regime appears with increasing gas velocity. The transition region is achieved from the slugging regime to the turbulent regime with progressive increase of the gas velocity. Also, it is possible to reach the turbulent regime from the bubbling regime, by-passing slugging fluidization, depending on the operation conditions and the type of particles (Bi and Grace, 1995; Zijerveld et al., 1998).

In the bubble regime, the bubbles flow up through the bed, and their coalescence and the explosion of the bubbles on the bed surface causes pressure fluctuations, while the dense phase continues as a compact zone. In the slugging regime, the diameter of the bubbles reaches the diameter of the column, causing the alternative passage of bubbles and the solid phase through the column. Slugging at high gas velocities produces a large bubble, or a train of large bubbles, that explode on the surface of the bed, which impels the solid particles upstream. Then, they fall and return to the bed, creating a strong periodic signal in the pressure fluctuations. The same, or similar, thing occurs in the region of transition; large bubbles passing through the bed impel the particles to the top of the column; then, they fall and return to the bed. This periodic motion is reflected in the pressure fluctuations, and the solids move intensely in both the disengaging zone and in the dense phase of the bed. The moment for the transition zone is more periodic and the unfolding process is slower compared with the bubble regime, which may be due to the structure of the bed at very intense fluidization. Passing the bubbles and the dense phase at a high velocity, without bubble coalescence, behaviour similar to that of the intense slugging flow is produced. For the bubbling regime, with many small bubbles and transport conditions, the flow distribution is more uniform and continuous in the bed and this behaviour can be seen in the plots.

The evolution of the moments calculated from the time series of pressure fluctuations obtained by Johnson et al. (2000) has been analysed. Those authors studied multiple bubble, single bubble, exploding bubble and the transport regimes observed in a $0.7 \text{ m} \times 0.12 \text{ m}$ cross-section bed using sand particles of $310 \mu\text{m}$ diameter. From each original time series, ten smaller time series of 4096 data values were generated by grouping the original data into windows. Fig. 3 reflects the evolution of the moment $M_{1,2}$. As shown, for the multiple bubble regime, the moment increases with the delay up to a maximum, then decreases, reaching a more or less constant value. The single bubble regime, which has a bed structure that is similar to slugging, also has similar moment evolution. An alternative unfolding and folding process is produced, and the degenerative process is much slower than in the bubble regime. In the exploding bubble regime, development is qualitatively similar to that of the slugging regime but with a lower period and it is qualitatively comparable to that of the intense slugging regime. The moment evolution in the transport regime is also similar to that in the multiple bubble regime; however, the periodic component is less intense.

After analysing the evolution of all moments for every time series of the pressure fluctuations studied, it is obvious that the evolution of the first interval of deployment is different for each flow regime, and it contains valuable information related to the fluidization regime. For this reason, Annunziato and Abarbanel (1999)

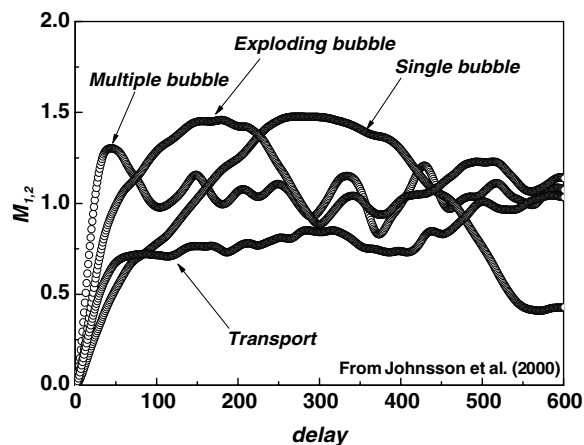


Fig. 3. Progress of the moment $M_{1,2}$ for the different regimes studied by Johnson et al. (2000).

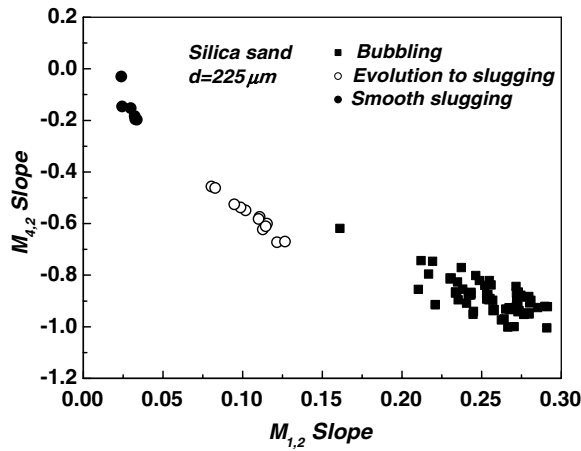


Fig. 4. Classification map using the unfolding descriptors, the slope of moments $M_{4,2}$ versus $M_{1,2}$ from bubbling to slugging regime for 225 μm diameter silica sand particles.

used this interval to classify gas–liquid flow regimes. But it is evident that the second zone, where the degradation process occurs, also has valuable information (but that is not used in this work). It has been observed that the slope of the moments in the first zone of its evolution has different values, according to the flow regime considered (Figs. 1–3). Therefore, the slope has been selected as the unfolding descriptor to classify the flow regimes.

Fig. 4 shows the plots of the slope of the moment $M_{4,2}$ versus the slope of $M_{1,2}$ for 225 μm diameter silica sand particles. As can be seen in this Fig. 4, each regime is located in a clearly different region of the map. A linear tendency is observed from bubbling to slugging, decreasing the absolute value of the moment slopes and approaching to the origin. This decrease of the absolute value of the slope is due to the decrease of the chaotic behaviour, since the non-periodic dynamic (bubbling) is more chaotic than the quasi-periodic (slugging).

An excellent classification of the bubble and turbulent regimes has been observed as shown in Fig. 5. The evolution is also linear, suggesting a decrease of the chaotic character from the bubbling regime to the turbulent regime, which is due to the more uniform structure of the bed compared to the structure of the bubbling bed, which has two different phases, bubbles and dense phase.

The moment slopes from the data of the four regimes studied by Johnson et al. (2000) are plotted in Fig. 6. The plot shows that the slopes of every regime are located in a defined region of the map following, as seen

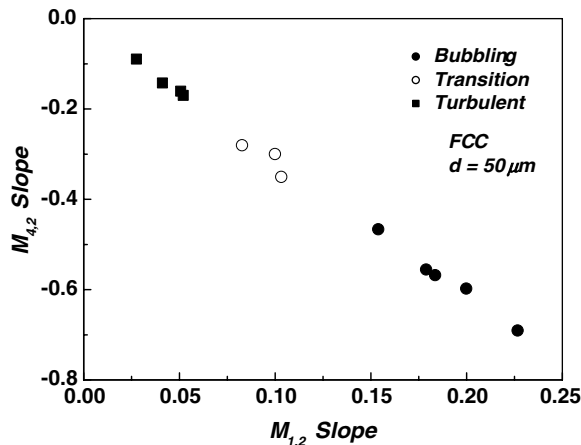


Fig. 5. Classification map from bubbling to turbulent regime for FCC 50 μm particles.

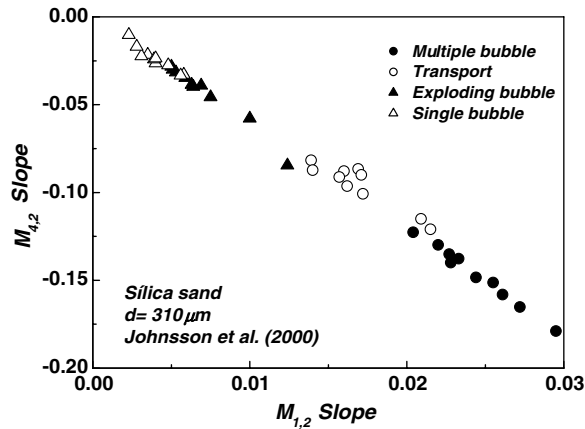


Fig. 6. Classification map for the regimes studied by Johnsson et al. (2000).

previously, a linear progression. The multiple bubbling regime (non-periodic motion), with the highest absolute values of the slope, has the most chaotic behaviour. The points corresponding to the single bubble regime (quasi-periodic motion) are at the opposite extreme because they have less chaotic behaviour. For the exploding bubble regime, the chaotic behaviour increases slightly, and for the turbulent regime, its increment is greater due to the loss of the periodic motion.

By carrying out an accurate analysis of the classification robustness for all the moments studied, we have observed some suitable descriptors that classify very well. This is the case of the moments slope $M_{1,2}$, $M_{1,4}$, $M_{2,2}$, $M_{2,4}$, $M_{4,2}$ and $M_{4,4}$, for which the classification is acceptable or excellent. While other descriptors ($M_{3,1}$, $M_{4,3}$, $M_{5,3}$ and $M_{6,2}$) are not suitable, because they give large errors, from 20% to 30%. Keeping in mind the general results, the method provides very good classification. From all the plots carried out with descriptor couples from the moments studied, 78.6% of classifications were between acceptable and excellent, 12.4% were acceptable (same dispersion is observed), and 9% were not acceptable.

5. Conclusions

A new methodology has been developed to characterize and classify fluidization regimes on the basis of chaotic analysis of pressure fluctuations in the bed. For each time series of pressure fluctuations, different attractors have been calculated: one for each delay.

Two different zones arise during the attractor evolution, which are reflected in the moment evolution. The first zone corresponds to the unfolding process, having valuable information about the fluidization dynamics that is characteristic for each flow regime. The second zone is a consequence of the degenerative process of the attractor, which loses coherence. The evolution of the moments is characteristic of each flow regime. In the bubbling regime, the unfolding and degenerative process takes place quickly. In contrast, in the slugging regime the evolution is slower and has a strong periodic component. For the turbulent regime, the evolution occurs between the bubbling regime and the slugging regime.

In the unfolding zone, the moment evolution versus the delay is linear; therefore, the slope of the moment has been chosen as the unfolding descriptor. Only two moment slopes are necessary to classify the flow regimes studied.

The descriptor has been shown to be an adequate classification tool. The dynamic moments used are characteristic of each regime investigated in this work and of those investigated by Johnsson et al. (2000). The moments satisfactorily classify these regimes.

Johnsson et al. (2000) used the Kolmogorov entropy and the correlation dimension to characterize the fluidization regimes. The attractor description based on these invariants involves an uncertain delay value, which must be known. The change of these invariants with the gas velocity was used as a criterion for the change of regime. However, these invariants cannot be used as parameters for regime classification, because there is a

possibility that equal values of these invariants may correspond to different regimes. In this work, we have obtained good results using a very small amount of data, 4096, while [Johnsson et al. \(2000\)](#) recommend 65 536 samples for the accuracy of the analysis.

With the methodology developed in this work, it is possible to characterize the fluidization regimes by state space analysis, making it unnecessary to know the value of the delay and the attractor of the system. Different attractors have been generated introducing the delay as a variable. The evolution of the attractor varying the delay has been characterized in the unfolding process by using the metric moments as unfolding descriptors. Only a couple of these invariant values are needed to identify the fluidization regimes and therefore to classify them. The challenge is to implement the classification calculation process in a computer program to monitor fluidized beds. Such a monitoring will enable to acquire the pressure data and calculate the unfolding descriptors on-line using only a few samples.

Acknowledgement

The authors thank Professor F. Johnsson from the Chalmers University of Technology (Sweden) for providing the time series of pressure fluctuations used in this work.

References

- Abarbanel, H.D.I., 1996. Analysis of observed chaotic data. Springer-Verlag, New York.
- Annunziato, M., Abarbanel, H.D.I., 1999. Nonlinear dynamics for classification of multiphase flow regimes. In: Proceedings of International Conference on Soft Computing, SOCO, Genova, Italy.
- Bai, D., Issangya, A.S., Grace, J.R., 1999. Characteristics of gas-fluidized beds in different flow regimes. *Ind. Eng. Chem. Res.* 38, 803–811.
- Bi, H.T., Grace, J.R., 1995. Flow regime diagrams for gas–solid fluidization and upwards transport. *Int. J. Multiphase Flow* 21, 1229–1236.
- Daw, C.S., Hallow, J.S., 1993. Evaluation and control of fluidization quality through chaotic time series analysis of pressure-drop measurements. *AIChE Symp. Ser.* 89, 103–122.
- Ellis, N., Briens, L.A., Grace, J.R., Bi, H.T., Lim, C.J., 2003. Characterization of dynamic behaviour in gas–solid turbulent fluidized bed using chaos and wavelet analyses. *Chem. Eng. J.* 96, 105–116.
- Esbensen, K.H., Halstensen, M., Lied, T.T., Saudland, A., Svaestuen, J., de Silva, S., Hope, B., 1998. Acoustic chemometrics – From noise to information. *Chemometr. Intell. Lab. Syst.* 44, 61–76.
- Fraser, A.M., Swinney, H.L., 1986. Independent coordinates for strange attractors from mutual information. *Phys. Rev. A* 33, 1134–1140.
- Johnsson, F., Zijerveld, R.C., Schouten, J.C., van den Bleek, C.M., Leckner, B., 2000. Characterization of fluidization regimes by time-series analysis of pressure fluctuations. *Int. J. Multiphase Flow* 26, 663–715.
- Karamavruç, A.I., Clark, N.N., 1997. Local differential pressure analysis in a slugging bed using deterministic chaos theory. *Chem. Eng. Sci.* 52, 357–370.
- Llop, M.F., Jand, N., 2003. The influence of low pressure operation on fluidization quality. *Chem. Eng. J.* 95, 25–31.
- Llop, M.F., Madrid, F., Arnaldos, J., Casal, J., 1996. Fluidization at vacuum conditions. A generalized equation for the prediction of minimum fluidization velocity. *Chem. Eng. Sci.* 51, 5149–5157.
- Makkawi, Y.T., Wright, P.C., 2002. Fluidization regimes in a conventional fluidized bed characterized by means of electrical capacitance tomography. *Chem. Eng. Sci.* 57, 2411–2437.
- Roux, J.C., Simoyi, H., Swinney, H.L., 1983. Observation of strange attractors. *Physica D* 8, 257.
- Takens, F., 1981. Detecting strange attractors in turbulence. In: Rand, D.A., Young, L.S. (Eds.), *Dynamical systems and turbulence, Lecture Notes in Mathematics*, 898. Springer-Verlag, Berlin, pp. 366–381.
- Villa, J., Guardiola, J., 2003. Free top fluidized bed surface fluctuations as a source of hydrodynamic data. *Powder Technol.* 134, 133–144.
- Zijerveld, R.C., Johnsson, F., Marzocchella, A., Schouten, J.C., van den Bleek, C.M., 1998. Fluidization regimes and transition from fixed bed to dilute transport flow. *Powder Technol.* 95, 185–204.